

Particle field digital holographic reconstruction in arbitrary tilted planes

D. Lebrun, A.M. Benkouider, S. Coëtmellec and M. Malek

UMR 6614 CORIA, Rouen University, Avenue de l'Université, Technopôle du Madrillet,
76801 Saint-Etienne du Rouvray, France

Denis.lebrun@coria.fr

<http://www.coria.fr>

Abstract: Digital holography is applied to the reconstruction of small particles in a plane whose orientation is arbitrary as specified by the user. The diffraction pattern produced by the particles is directly recorded by a conventional CCD camera. The digital recorded image enables the recovery of particle-images in several parallel planes of the probe volume. Afterwards, an interrogation slice corresponding to a thin layer around a theoretical arbitrary tilted plane is fixed. The pixels whose 3D coordinates belong to this slice are selected and juxtaposed to rebuild the particle images. The feasibility is demonstrated on a fiber tilted with respect to the camera plane. A second example is given on an experimental particle field. These results let us predict future applications such as the characterization of particle fields in planes other than those parallel with the camera plane.

©2003 Optical Society of America

OCIS codes: (090.0090) Holography; (090.1760) Computer holography; (100.3010) Image reconstruction techniques; (100.6890) Three dimensional image processing

References and links

1. T.M. Kreis, W.P.O. Jüptner, "Suppression of the dc term in digital holography," *Opt. Eng.* **36**, 2357-2360 (1997)
2. M.K. Kim, "Tomographic three-dimensional imaging of a biological specimen using wavelength-scanning digital interference holography," *Opt. Express* **7**, 305-310, (2000)
<http://www.opticsexpress.org/abstract.cfm?URI=OPEX-7-9-305>
3. O. Schnars and W. Juptner, "Direct recording of holograms by a CCD target and numerical reconstruction," *Appl. Opt.* **33**, 179-181 (1994)
4. Yamaguchi and T. Zhang, "Phase-shifting digital holography," *Opt. Lett.* **22**, 1268-1270, (1997)
5. S. Belaïd, D. Lebrun and C. Özkul, "Application of two dimensional wavelet transform to hologram analysis: visualization of glass fibers in a turbulent flame," *Opt. Eng.* **36**, 1947-1951 (1997)
6. C. Buraga-Lefebvre, S. Coëtmellec, D. Lebrun and C. Özkul, "Application of wavelet transform to hologram analysis : three-dimensional location of particles," *Optics and Lasers in Eng.* **33**, 409-421 (2000)
7. L. Onural, "Diffraction from a wavelet point of view," *Opt. Lett.* **18**, 846-848, (1993)
8. S. Coëtmellec, D. Lebrun and C. Özkul, "Characterization of diffraction patterns directly from in-line holograms with the fractional Fourier Transform," *App. Optics*, **41**, 312-319, (2002)
9. S. Coëtmellec, C. Buraga-Lefebvre, D. Lebrun and C. Özkul, "Application of in-line digital holography to multiple plane velocimetry," *Meas. Sci and Tech.* **12**, 1392-1397 (2001)
10. S. Coëtmellec, D. Lebrun and C. Özkul, "Application of two-dimensional fractional-order Fourier transformation to particle field digital holography," *J. Opt. Soc. Am. A.*, **19**, 1537-1546, (2002)
11. L. Yu, Y. An and L. Cai, "Numerical reconstruction of digital holograms with variable viewing angles," *Opt. Express* **10**, 1250-1257, (2002)
<http://www.opticsexpress.org/abstract.cfm?URI=OPEX-10-22-1250>

1. Introduction

Digital holography has now largely replaced conventional holography and there are a significant number of publications concerning the numerical reconstruction of digital

holograms [1-4]. With the recent development of CCD cameras, it is now possible to record holograms in real-time. For a few years, it has been known that the 3-D location of particles or fibers can be accurately determined by numerical reconstruction of holograms that are directly recorded by a camera [5,6]. Recently, it has been shown that the reconstruction process can be seen either as a wavelet transformation or as a Fractional Fourier transformation of the intensity distribution recorded by the hologram [7,8]. The in-line configuration is convenient for metrology in fluids where optical access is not easy. Numerous papers have been published about the applications of Digital in-line holography such as velocimetry or particle field holography [9,10]. These methods allow the characteristics of a seeded flow (particle size, velocity vector fields) to be determined at a given time. In these applications, the images are only reconstructed in planes parallel with that of the sensor plane (vertical planes). However, in most cases it would be interesting to investigate other sections such as non-vertical planes, as has recently been proposed by L. Yu *et al.* [11]. The aim of this publication is not to present a novel reconstruction method but to demonstrate that the selective numerical reconstruction in tilted slices may be helpful in visualizing particles. First, the method used for digital reconstruction is presented. Then, in the following section, we give an example of the reconstruction of a tilted fiber. This example highlights the advantages of a selective reconstruction for visualization. Finally, the case of an experimental particle field is presented.

2. Digital reconstruction of in-line holograms

Let us recall the theoretical formalism developed by the author of Ref. [7] and the digital reconstruction process proposed in Ref. 6. Consider an object plane illuminated by a monochromatic plane wave (see Fig. 1).

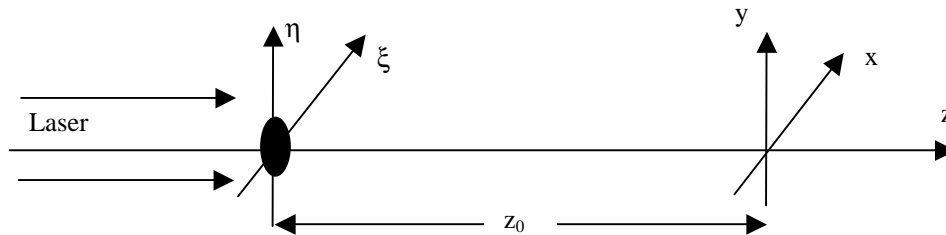


Fig. 1. Hologram recording in the Gabor configuration

For an opaque object, the amplitude distribution in the object plane is described by the function $[1-O(\xi,\eta)]$ where :

$$\begin{aligned} O(\xi, \eta) &= 1 \text{ if } (\xi, \eta) \text{ belongs to the object} \\ &= 0 \text{ elsewhere} \end{aligned}$$

The intensity distribution recorded on a plane (x,y) located at a distance z_0 from the object can be expressed as the following convolution product :

$$I_{z_0}(x, y) = 1 - O(x, y) * \frac{2}{\lambda z_0} \sin \left[\frac{\pi(x^2 + y^2)}{\lambda z_0} \right] \quad (1)$$

Here, note that the intermodulation term has been dropped. In fact, it is shown that when large recording distances are considered such that $z_0 \gg \pi d^2/\lambda$ where d is the object diameter, this term can be treated as a constant and can be neglected [5].

The expression given by Eq. (1) can be rewritten as a wavelet transform (WT) of the amplitude distribution in the object plane as follows :

$$I_{z_0}(x, y) = I - \frac{2}{\pi} WT_O(a_0, x, y) \quad (2)$$

The daughter wavelet functions are defined for the scale parameter a by :

$$\psi_a(x, y) = \frac{1}{a^2} \sin\left(\frac{x^2 + y^2}{a^2}\right) \quad (3)$$

The scale parameter a_0 of the wavelet is related to the distance z_0 as follows :

$$a_0 = \sqrt{\frac{\lambda z_0}{\pi}} \quad (4)$$

In the same way, this approach can be used for hologram reconstruction. The reconstructed image at a given distance z_r can be seen as the WT of the intensity distribution recorded by the photosensitive plane : $WT_{I_{z_0}}(a_r, x, y)$. When $a_r = a_0$ (i.e. the interrogation plane located at a distance z_r corresponds to the object plane located at a distance z_0), it can be shown that by dropping a multiplicative constant :

$$WT_{I_{z_0}}(a_0, x, y) = I - O(x, y) - \frac{1}{2\lambda z_0} O(x, y) ** \sin\left[\frac{\pi(x^2 + y^2)}{2\lambda z_0}\right] \quad (5)$$

The reconstructed image corresponds to the second term of the right side of Eq. (5). The third term can be interpreted as the well-known fringes due to the twin image located at a distance $2z_0$ from the reconstruction plane. More details can be found in Ref. [5].

3. Digital reconstruction in a tilted plane

The method recalled in Section 2 could easily be applied to the numerical reconstruction in planes that are not parallel with respect to the detector plane. Knowing that the information concerning the whole volume is contained in the diffraction pattern, the digital reconstruction along a tilted plane consists in selecting useful information from multiple reconstructed planes. This process is nothing more than using a variable scale parameter a_r in Eq. (5).

In order to highlight the benefit of such a process, a simple situation concerning a simulated tilted fiber is considered here. Let us consider a small and straight fiber belonging to the (η, z) plane and making an angle θ_0 with respect to the η direction (see Fig. 2).

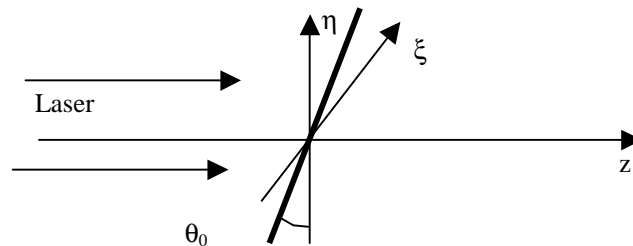


Fig. 2. Geometrical configuration for a tilted fiber

This fiber is considered here as a succession of vertical fiber elements, each element being located at a distance z_0 from the CCD camera. If we assume that the diffraction pattern produced by the fiber is the contribution given by each fiber element, the intensity distribution in the diffraction pattern $I(x,y)$ is given by Eq. (1) where $z_0 = D_0 + y \tan \theta_0$. D_0 is the distance between the fiber and the camera for $y=0$.

Figure 3a shows a simulation of the diffraction pattern $I(x,y)$ produced by a fiber of diameter $d=60 \mu\text{m}$ which is illuminated by a plane wave of wavelength $\lambda = 0.6328 \mu\text{m}$ and where $\theta_0 = 84,2^\circ$. This figure consists of a 512×512 array of 256 gray level pixels. The parameters d and θ_0 have been chosen in order to highlight the variations of the diffraction pattern along y axis. On this example, z_0 lies in the interval $[50, 95 \text{ mm}]$. As we can see here, the width of the central fringe grows as the distance z_0 increases. Figure 3b shows the image obtained by applying to the diffraction pattern $I(x,y)$ the reconstruction formulae given by Eq. (5) ($WT_I(a_r, x, y)$) and for $z_r = D_0$. Here, except for $y=0$, the condition $z_r = z_0$ is not satisfied. Consequently, the reconstruction process seen as a wavelet transform is only valid for the pixels located on the line $y=0$. As we can see on Fig. 3b, $WT_I(a_r, x, y)$ leads to a satisfactory reconstruction only in the central region of the figure. This focusing process reveals itself by a narrowing of the central fringe. Observe that the image is in focus along 1 mm in the y direction. Consequently, the reconstructed images presented in this paper represent a slice rather than a plane. The thickness of a given slice depends on the depth of field given by the numerical reconstruction (see Ref. [9]).

In order to visualize another fiber element not necessarily located at $z_0=D$, $WT_I(a_r, x, y)$ should be computed with a scale parameter in accordance with the reconstruction in another plane. Thus, by combining all the reconstructed images, the totality of the fiber portion corresponding to the field seen by the camera could be analyzed. These operations can be synthesized in the following two-step process : 1 - Reconstruction plane by plane of the whole volume for different values of z_r , 2 - Rebuilding of the intensity in a tilted direction by selecting within a given z_r -plane the pixels belonging to this plane (i.e we hold in a given z_r -plane only the pixels whose coordinates verify : $z_r = D_0 + y \tan \theta_0$). An example of reconstruction is given in Fig. 3c. Observe that the lateral fringes due to the twin image move away as z_r increases.

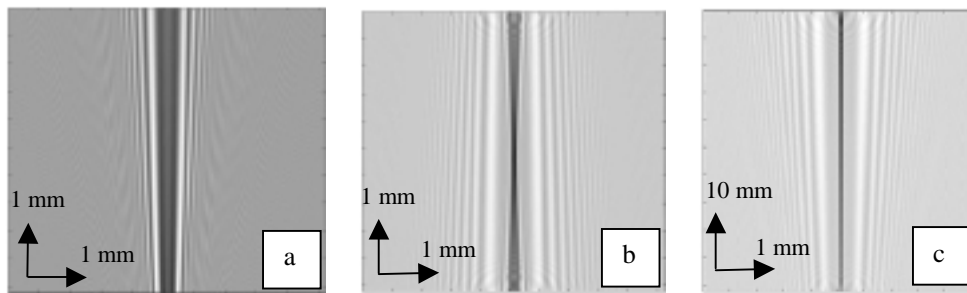


Fig. 3. Reconstruction in a tilted plane. (a) Intensity distribution in the diffraction pattern for a tilted fiber ($d= 60 \mu\text{m}$, $D_0= 73 \text{ mm}$ and $\theta_0 = 84.2^\circ$), (b) image reconstructed at $z_r=D_0$ and (c) image reconstructed in the fiber plane by selecting the pixels owing to this plane

4. Experimental results

This method has been applied to an experimental case where a fiber of diameter $d=30 \mu\text{m}$ is illuminated by a collimated laser source ($\lambda=0.6328 \mu\text{m}$). The diffraction pattern presented on Fig. 4a is recorded and digitized by a standard CCD camera connected to a computer vision system. The fiber is not perfectly straight but makes a mean angle $\theta_0 = 67^\circ$ with respect to the y direction. The central fiber element is located at a distance $D_0 = 40 \text{ mm}$ from the CCD sensor. Figure 4b is obtained by applying the digital reconstruction formula given by the Eq. (5) for $z_r = 50 \text{ mm}$. Note that, as is the case for the numerical simulations, the image of the

fiber is only focused in a small region of the image (top of the figure). The image in Fig. 4c has been calculated by applying a numerical reconstruction process to the whole volume contained between $z_r = 30$ mm and $z_r = 50$ mm. Afterwards, we selected only the pixels that verify $z_r = D_0 + y \tan \theta_0$. The fiber is well reconstructed within the whole field of view but the contrast at the center of the image decreases for the smallest values of z_r . This can be explained by the windowing function applied on the daughter wavelet $\psi_{ar}(x, y)$ for the reconstruction. Indeed, for an object located near the CCD camera, a_r takes smaller values, so the windowing function must be narrowed enough to verify the spatial sampling condition (see Ref. 5). Consequently, the number of side lobes of the diffraction pattern involved in the digital reconstruction process is reduced and the contrast of the images is reduced too.

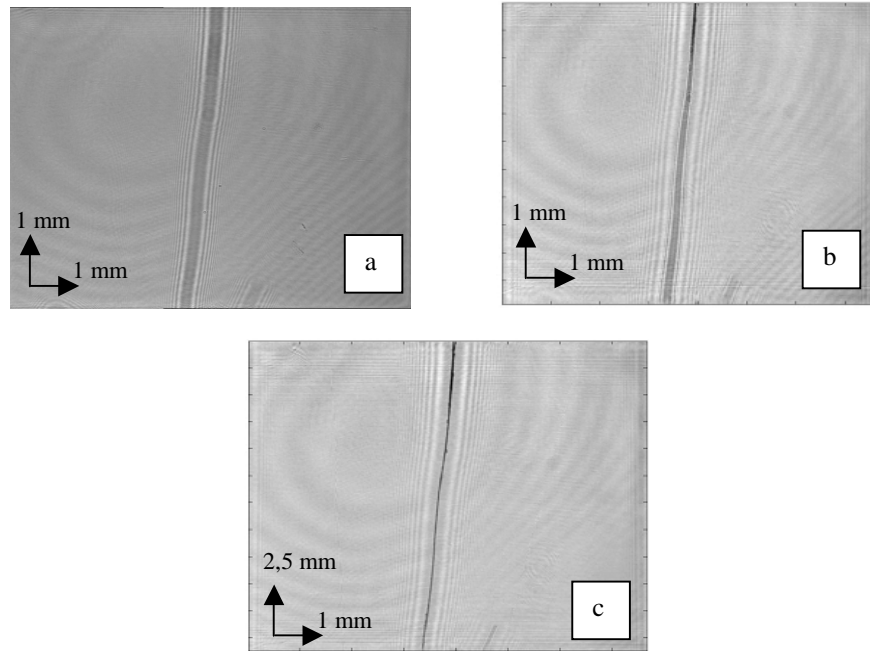


Fig. 4. Reconstruction in a tilted plane, experimental results. (a) Intensity distribution in the diffraction pattern for a tilted fiber ($d= 30 \mu\text{m}$, $D_0= 40$ mm and $\theta_0 = 67^\circ$), (b) image reconstructed at $z_r=50$ mm, (c) image reconstructed in the fiber plane by selecting the pixels owing to this plane

This method also leads to significant results when applied to a particle field. The example schematized by Fig. 5 concerns liquid droplets produced by a spray nozzle (swirl injector). The droplets are mainly located within a volume of 40 mm in depth. The source used here is a Nd:Yag laser emitting at $\lambda= 532$ nm. This laser is commonly used in our laboratory for Particle Image Velocity (PIV) experiments. Figure 6a corresponds to the diffraction patterns recorded directly by the CCD camera. Figure 6b is the digital reconstruction in a plane parallel to the CCD plane at $z_r = 120$ mm. We can see that one of the particle images indicated by dashed arrows is in focus (upper left corner) whereas the other image at the bottom of the figure is defocused. The image shown in Fig. 6c has been obtained by adjusting the two parameters (D_r, θ_r) such that these particle images are both focused. We found $D_r=100$ mm and $\theta_r = 76^\circ$. Note that this example exhibits a singular case where nearly all the droplet images belong to the same slice.

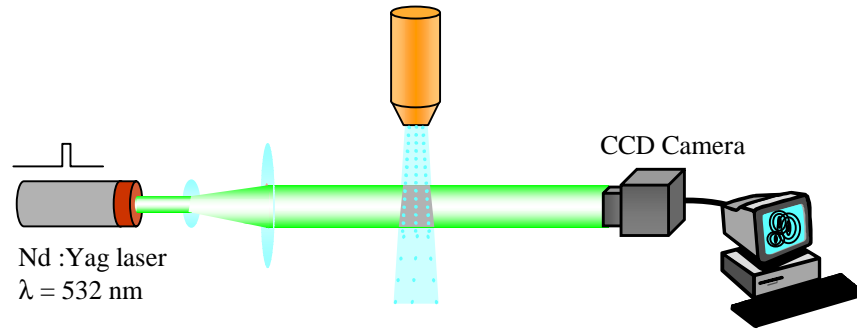


Fig. 5. Experimental recording setup

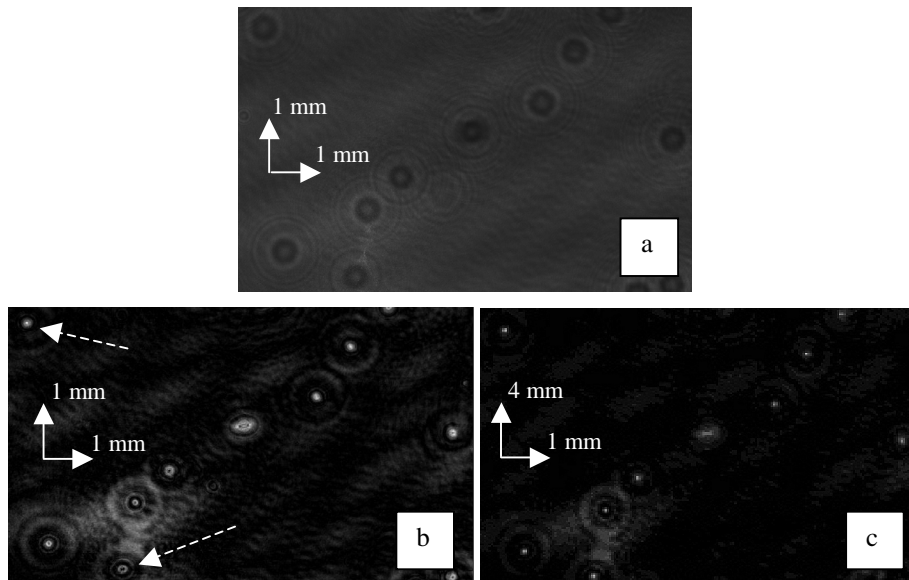


Fig. 6. Experimental results on a particle field produced by a spray : (a) diffraction pattern recorded by the CCD camera, (b) image reconstruction at $z_r = 120$ mm, (c) image reconstruction on a tilted plane ($D_r = 100$ mm, $\theta_r = 76^\circ$)

5. Conclusion

A probe volume reconstructed by digital holography is processed in order to rebuild the intensity distribution of particle images located in slices oriented by a user. The feasibility is demonstrated on a straight fiber whose main direction is not parallel with respect to the CCD plane. Some experimental results are given for liquid droplets produced by a spray. We show that by using this method, it is not necessary to scan multiple planes to reconstruct simultaneously several images located in different z -planes. This point may be appreciated in the field of particle diagnostics and particularly in velocity measurements. For example, the characterization of a velocity vector field in a given tilted slice can be envisaged. Moreover, it must be emphasized that only one camera without an objective is needed for the recording setup. This is another advantage for fluid mechanics measurements where optical access is sometimes limited.